

# Search for MSSM/mSUGRA at DØ

Martin Wegner, for the DØ collaboration

III. Physik. Inst. A, RWTH Aachen, Germany

Received: 3 November 2003 / Accepted: 19 November 2003 /  
Published Online: 3 December 2003 – © Springer-Verlag / Società Italiana di Fisica 2003

**Abstract.** This report summarizes recent searches for supersymmetric particles using the DØ Detector at Fermilab. Limits on the production of stop squarks are reported. The status of the mSUGRA search for  $\chi^0\chi^\pm \rightarrow ll$  and of a model-independent search for  $e + \mu$  final states are presented. The first evidence for  $\tau$  identification in the DØ Run II data is shown.

## 1 Introduction

Supersymmetry (SUSY) is a hypothetical fundamental space-time symmetry transforming fermions into bosons and vice versa [1]. As a consequence the particle spectrum is doubled, i.e. there is a supersymmetric partner to every Standard Model particle. The scenario consisting only of the SM particles, its corresponding super-partners and two Higgs doublets is referred to as “Minimal Supersymmetric Extension of the Standard Model” (MSSM).

Spontaneous SUSY breaking at the Planck scale can be achieved in theories of supergravity. In its minimal version (mSUGRA), in which electroweak symmetry breaking is radiatively induced, the free parameters are reduced to universal scalar and gaugino masses  $m_0$  and  $m_{1/2}$ , a universal trilinear coupling  $A_0$ , the ratio of the Higgs VEVs  $\tan\beta$  and the sign of the Higgs mass parameter  $\mu$ .

## 2 Tevatron and the DØ experiment

The proton-antiproton collider “Tevatron” near Chicago underwent a major upgrade from “Run I” to “Run II” in the years 1997-2001, where the beam energy was raised from 1.8 TeV to 1.96 TeV. At the same time the number of bunches was increased from  $8 \times 8$  to  $36 \times 36$  leading to a higher luminosity [2]. Between spring 2001 and July 2003 approx.  $260 \text{ pb}^{-1}$  were delivered, compared to  $110 \text{ pb}^{-1}$  before the upgrade.

To be ready for higher occupancies, several parts of the two detectors CDF and DØ were replaced or modified. The DØ detector is now equipped with new fine-segmented muon chambers in the end-caps, additional muon trigger counters, a new central tracking system (consisting of a 2 T solenoid magnet, a silicon vertex detector and a scintillating fiber tracker) and new calorimeter electronics. Furthermore a new 3-level trigger and a new data acquisition system were commissioned.

## 3 Stop search in Run I data

For this analysis we assume the stop ( $\hat{t}$ ) to be the next-to-lightest supersymmetric particle which decays 100% to a charm quark and the lightest neutralino.

### 3.1 Background

The potential signal is superimposed by large Standard Model backgrounds, mainly from W- and Z-decays where either a quark is produced or a charged lepton is misidentified as a jet. In detail, the dominant Standard Model backgrounds are:

- $W \rightarrow l\nu + \text{jets}$
- $W \rightarrow l\nu, W \rightarrow qq$
- $W \rightarrow l\nu, Z \rightarrow \text{anything}$
- $Z \rightarrow \tau\bar{\tau}$
- $Z \rightarrow \nu\bar{\nu}$
- $t\bar{t}$  decays.

In addition detector mis-measurements and inefficiencies can lead to fake missing transverse energy.

### 3.2 Data set and cuts

A total of  $85.2 \text{ pb}^{-1}$  of Run I data [4] was taken with a di-jet+ $\cancel{E}_T$  trigger. To improve the signal to background ratio, the  $p_T$  of the leading jet was required to be above 100 GeV, the second jet to be above 60 GeV and the missing transverse energy to be above 40 GeV. In order to reduce the amount of mis-measured  $\cancel{E}_T$  the polar angle between any jet and the missing  $E_T$  had to be greater than  $30^\circ$ . Furthermore jets in the overlap region of central and end-cap calorimeters were not used. The leading jet was required to be in the central calorimeter ( $\eta < 0.6$ ).

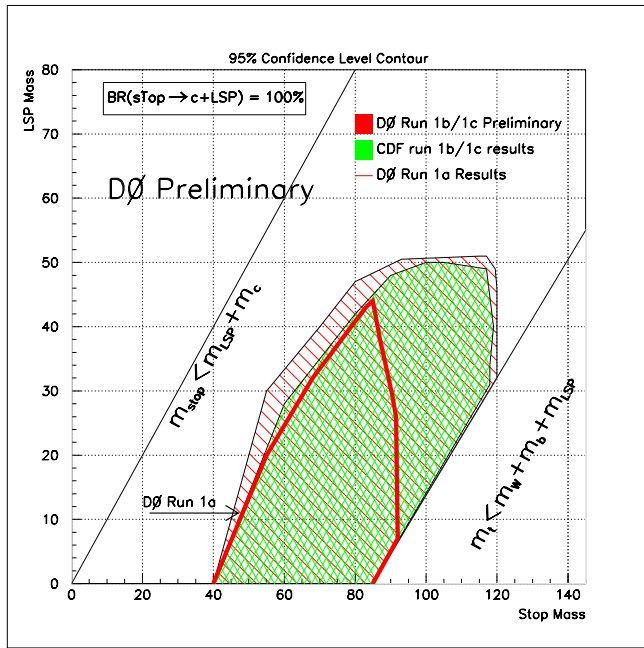


**Fig. 1.** 95% C.L. exclusion region in the  $m_{\tilde{t}} - m_{LSP}$  plane for the case  $BR(\tilde{t} \rightarrow c + LSP) = 100\%$

### 3.3 Results

After all cuts 12 events remained, which is consistent with the  $12.81 \pm 1.77$  events being expected from background. This absence of an excess in signal events can be translated to an excluded region in the  $m_{LSP} - m_{\tilde{t}}$  plane. As shown in Fig. 1 these results improve the limits of previous Tevatron analyzes.

## 4 Chargino/neutralino search in the 3-lepton channel

In proton-proton collisions the lightest chargino and the second-lightest neutralino are typically produced associated. While the  $\chi_2^0$  can decay into a  $\chi_1^0$  (LSP) and via a  $Z^*/\gamma^*$  or a  $f$  into a lepton-pair, the  $\chi_1^\pm$  can decay into a  $\chi_1^0$  and via a  $W^*$  into a charged lepton and a neutrino [5]. In R-Parity conserving scenarios the LSP is stable and escapes the detector. The interesting signal therefore consists of three charged leptons plus missing energy. This three-lepton final state particularly excels by its low Standard Model background.

In the present analysis we search for two identified electrons and a third isolated track.

### 4.1 Signal and background

Two mSUGRA parameter sets ( $m_0 = 500$  GeV,  $m_{1/2} = 100$  GeV,  $\tan\beta = 2$ ,  $\mu > 0$  and  $m_0 = 150$  GeV,  $m_{1/2} = 150$  GeV,  $\tan\beta = 2$ ,  $\mu > 0$ ) were chosen to generate Monte Carlo events. The  $ee$  invariant mass distributions show peaks between 30 and 60 GeV, i.e. below the  $Z$ -mass region.

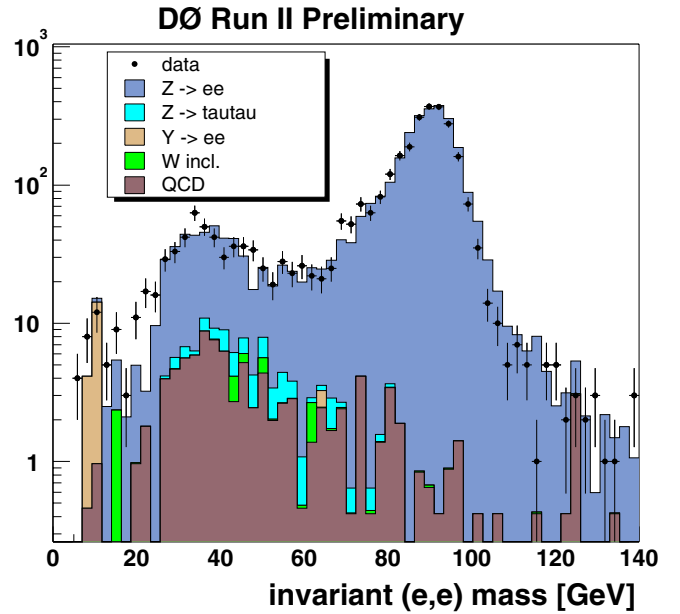


**Fig. 2.** Invariant di-electron mass distribution from data (dots with error bars) and from simulated backgrounds (histograms) for events with two identified electrons, one with  $p_T > 15$  GeV

The background to this channel mainly consists of those Standard Model processes with at least one electron in the final state; the second electron can be feigned by a mis-identified jet or a photon with a coincidental track match. Figure 2 shows that the initial DØ data set, only requiring two identified electrons (or positrons), can be understood well by the known backgrounds.

Cutting on the invariant  $ee$ -mass ( $10 \text{ GeV} < m_{ee} < 70 \text{ GeV}$ ) and the transverse  $e - \cancel{E}_T$  mass and requiring a third isolated track, removes all but two candidates, while about 50% of the signal Monte-Carlo remains. Requiring additionally a missing transverse energy above 15 GeV leaves 0 events while  $0 \pm 2$  are expected from the SM. This corresponds to a 95% C.L. limit of  $\sigma_{\text{prod}} \times BR = 3.54$  pb for the first and  $\sigma_{\text{prod}} \times BR = 2.20$  pb for the second mSUGRA parameter set.

## 5 Tau identification in Run II

In the case of larger  $\tan\beta$  the branching ratio of  $\chi^\pm/\chi^0$  into light leptons decreases and therefore  $\tau$  identification becomes crucial. In the following an approach is described to identify hadronically decaying taus using a neural network. Here we are looking for  $Z \rightarrow \tau\tau$  with one of the taus decaying into an electron and the other one into a one-prong hadronic jet.

Seven variables characterizing the longitudinal profile of the calorimeter clusters or combined information from the tracker and the calorimeter are used as input for the neural network. Among the candidates selected by this NN, those are discarded, which are compatible with the hypothesis of a “loose” electron. To remove low- $p_T$  QCD jets, only  $\tau$  candidates with  $p_T > 7$  GeV are accepted.

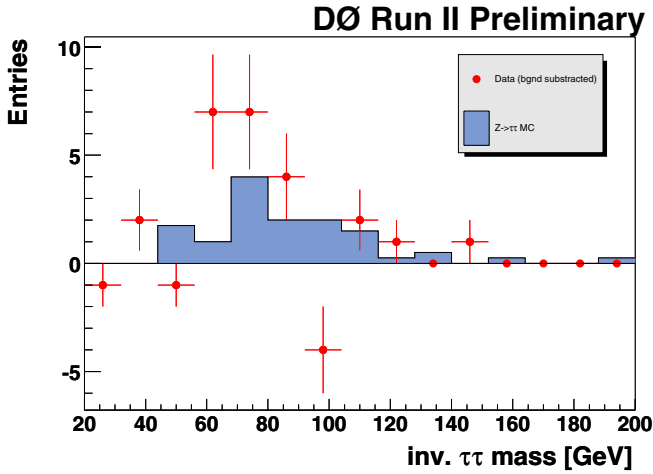


Fig. 3. Difference between like-sign and unlike-sign  $\tau$  candidates after all cuts (dots with error bars) and signal MC expectation for  $\mathcal{L} = 50 \text{ pb}^{-1}$

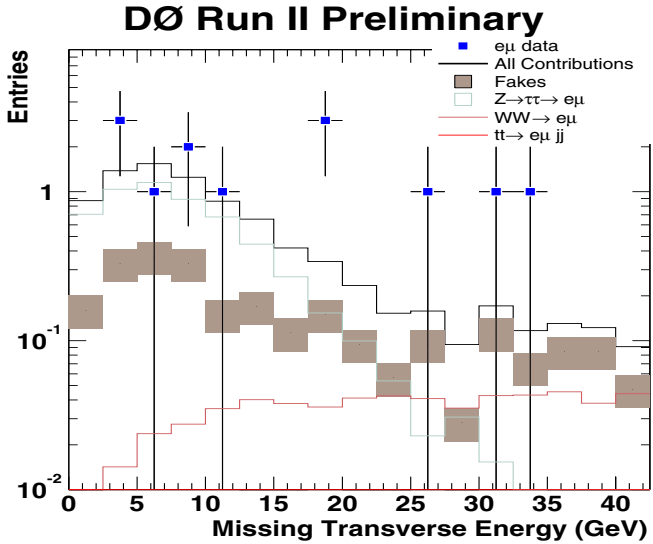


Fig. 4. Distribution of  $\cancel{E}_T$  for  $e\mu$  events after all cuts (dots with error bars) and background expectation (histograms)

Cuts on the invariant  $e - \cancel{E}_T$  and  $e - \tau$  masses are imposed to exclude  $W \rightarrow e\nu$  and  $Z \rightarrow ee$  events, where the electron is mis-identified as  $\tau$ . By assuming that the  $\tau$  directions are given by the directions of the visible decay products ( $e$  and jet), by using the  $\cancel{E}_T$ -measurement correction factors to  $p_T^{\text{jet}}$  and  $p_T^e$  can be calculated to reconstruct the original  $\tau$  momenta (collinear approximation). Events with an  $e$  and a jet back-to-back are excluded.

The invariant mass distribution of the observed  $\tau$  candidates which is based on an integrated luminosity of  $\mathcal{L} = 50 \text{ pb}^{-1}$  (Fig. 3), shows a peak with an excess of unlike-sign events in the mass range of 60–110 GeV which is the first evidence for a successful  $\tau$ -identification at DØ.

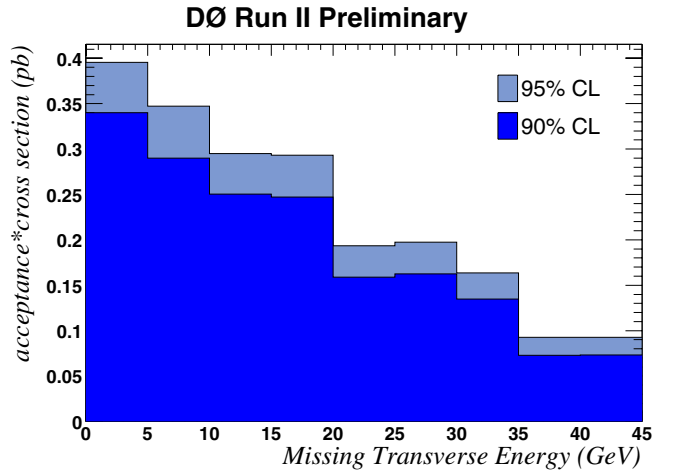


Fig. 5. Limits for the product of acceptance  $\times$  cross section for the  $e + \mu$  signature versus missing transverse energy. (For comparison: The acceptance for  $WW \rightarrow e\mu$  is 16.9 %)

## 6 Model-independent search in the $e\mu$ -channel for Run II

Since the channel  $p\bar{p} \rightarrow e\mu + X$  has only a very small cross-section in the Standard Model, it is sensitive to several scenarios of new physics where events of this kind are predicted. It is therefore well suited for a model-independent search for deviations from SM predictions. The present analysis uses an integrated Luminosity of  $\mathcal{L} = 33 \text{ pb}^{-1}$  of Run II data.

The dominant backgrounds are  $Z/\gamma^* \rightarrow \tau\tau \rightarrow e\mu\nu\nu$ ,  $WW \rightarrow e\mu\nu\nu$  and  $tt \rightarrow e\mu\nu\nu jj$ . While the  $Z$ -background shows a lower lepton  $p_T$  and  $\cancel{E}_T$  than the rest, the  $WW$  and  $tt$  backgrounds differ in the average number of jets.

As shown in Fig. 4 the  $e\mu$  candidates remaining after all cuts are fully compatible with the Standard Model predictions. This can be translated into a model-independent limit on the product of cross sections times acceptance as a function of  $\cancel{E}_T$  (Fig. 5).

## References

1. S.P. Martin: hep-ph/9709356 (1997) and references therein
2. S. Abachi et al.: Nucl. Instrum. Meth. A **408**, 103–109 (1998)
3. R. Demina, J.D. Lykken, K.T. Matchev, and A. Nomeroski: Phys. Rev. D **62**, 035011 (2000)
4. S. Abachi et al.: Nucl. Instr. Meth. A **338**, 185 (1994)
5. H. Baer and X. Tata: Phys. Rev. D **47**, 2739–2745 (1993)